

## **Diagnostics and Modeling of the Auroral Ionosphere Under the Influence of the Gakona HF Transmitter**

**Davis D. Sentman**

**Geophysical Institute  
University of Alaska Fairbanks  
903 Koyukuk Drive  
Fairbanks Alaska 99775**

**August 2001**

**APPROVED FOR PUBLIC RELEASE; DISTRIBUTION UNLIMITED.**

**20021031 036**



**AIR FORCE RESEARCH LABORATORY  
Space Vehicles Directorate  
29 Randolph Rd  
AIR FORCE MATERIEL COMMAND  
Hanscom AFB, MA 01731-3010**

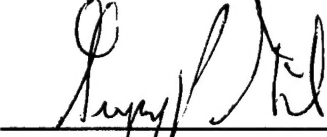
---

"This technical report has been reviewed and is approved for publication"



---

JAMES C. BATTIS  
Contract Manager



---

GREGORY P. GINET  
Branch Chief

This report has been reviewed by the ESC Public Affairs Office (PA) and is releasable to the National Technical Information Service (NTIS).

Qualified requestors may obtain additional copies from the Defense Technical Information Center (DTIC). All others should apply to the National Technical Information Service (NTIS).

If your address has changed, if you wish to be removed from the mailing list, or if the addressee is no longer employed by your organization, please notify AFRL/VSIP, 29 Randolph Road, Hanscom AFB, MA 01731-3010. This will assist us in maintaining a current mailing list.

Do not return copies of this report unless contractual obligations or notices on a specific document require that it be returned.

REPORT DOCUMENTATION PAGE					Form Approved OMB No. 0704-0188	
<p>The public reporting burden for this collection of information is estimated to average 1 hour per response, including the time for reviewing instructions, searching existing data sources, gathering and maintaining the data needed, and completing and reviewing the collection of information. Send comments regarding this burden estimate or any other aspect of this collection of information, including suggestions for reducing the burden, to Department of Defense, Washington Headquarters Services, Directorate for Information Operations and Reports (0704-0188), 1215 Jefferson Davis Highway, Suite 1204, Arlington, VA 22202-4302. Respondents should be aware that notwithstanding any other provision of law, no person shall be subject to any penalty for failing to comply with a collection of information if it does not display a currently valid OMB control number.</p> <p><b>PLEASE DO NOT RETURN YOUR FORM TO THE ABOVE ADDRESS.</b></p>						
1. REPORT DATE (DD-MM-YYYY) 23 August 2001		2. REPORT TYPE Scientific & Technical Report #1		3. DATES COVERED (From - To) July 29, 1999 to January 31, 2001		
4. TITLE AND SUBTITLE  Diagnostics and Modeling of the Auroral Ionosphere under the influence of the Gakona HF Transmitter			5a. CONTRACT NUMBER F19628-99-C-0059  5b. GRANT NUMBER  5c. PROGRAM ELEMENT NUMBER 62601F  5d. PROJECT NUMBER 4266  5e. TASK NUMBER GH  5f. WORK UNIT NUMBER AJ			
6. AUTHOR(S) Sentman, Davis D. Wescott, Eugene M. Olson, John V. Otto, Antonius Bristow, William A. Solie, Daniel J. Petersen, John K.			8. PERFORMING ORGANIZATION REPORT NUMBER			
7. PERFORMING ORGANIZATION NAME(S) AND ADDRESS(ES) Geophysical Institute University of Alaska Fairbanks 903 Koyukuk Drive Fairbanks, AK. 99775-7230			10. SPONSOR/MONITOR'S ACRONYM(S)			
9. SPONSORING/MONITORING AGENCY NAME(S) AND ADDRESS(ES) Air Force Research Laboratory 29 Randolph Road Hanscom Air Force Base, MA 01731-3010 Contract Manager: James Batis, VSBX1			11. SPONSOR/MONITOR'S REPORT NUMBER(S) AFRL-VS-TR-2001-1622			
12. DISTRIBUTION/AVAILABILITY STATEMENT Approved for public release; distribution unlimited						
13. SUPPLEMENTARY NOTES						
14. ABSTRACT <p>This project comprises five separate elements that address science and education objectives of the HAARP program. These elements are: 1. To establish the characteristics of the ionospheric source region responsible for the ELF/VLF waves generated by modulation of HAARP HF emissions, and to measure the ELF radiation pattern. 2. To attempt to stimulate hydromagnetic waves in the ionospheric wave-guide using the HAARP heater. 3. To develop a simulation model for the plasma physical and electromagnetic effects of localized ionospheric heating with the purpose of predicting outcomes of heating experiments and to guide the design of new experiments. 4. Using the SuperDARN instrument on Kodiak, to examine the formation of ionospheric irregularities within the heated volume and the relationship of the irregularities to other observations such as the generation of Stimulated Electromagnetic Emissions. 5. To provide scientific education about HAARP and physical science in general to members of the local Copper Valley community. In this report the results of research obtained to date in each of the five program elements are reviewed, and recommendations for follow up activities are presented.</p>						
15. SUBJECT TERMS HAARP, Ionosphere, Diagnostics, Modelling						
16. SECURITY CLASSIFICATION OF: a. REPORT unclassified		17. LIMITATION OF ABSTRACT b. ABSTRACT unclassified c. THIS PAGE unclassified		18. NUMBER OF PAGES 33	19a. NAME OF RESPONSIBLE PERSON Davis D. Sentman  19b. TELEPHONE NUMBER (Include area code) 907-474-6442	

## CONTENTS

<b>Contents.....</b>	iii
<b>List of Figures and Tables .....</b>	iv
<b>Reports on Program Elements .....</b>	1
<b>Element:</b>	
1. ELF/VLF Wave Measurement and Interpretation Program and 1a. Survey and Characterization of HAARP Antenna Pattern .....	1
2. ULF Wave Measurement Program .....	17
3. Auroral Ionosphere Modeling Program.....	20
4. SuperDARN Operations.....	25
5. HAARP Science Outreach .....	30
<b>References .....</b>	32
<b>Symbols, Abbreviations, Acronyms .....</b>	33

## FIGURES AND TABLES

<b>Figures</b>	<b>Page</b>
1. Sensor box sensors and instrument trailer at Gakona ELF site.	2
2. Synchronously detected signals 256-4000 Hz in Bx during the Fall 2000 campaign.	5
3. Resistivity vs. depth calculated using the Bostick algorithm derived from the modulated HAARP signal.	7
4. Remote field sites used for antenna pattern measurements, plus the Gakona reference site, indicated in red. The HAARP location is indicated in gold. The legend at the right refers the site designations to their names.	8
5. Amplitude in pT of the By magnetic component of synchronously detected HAARP signals obtained 14 Sep 2000 from Cordova, 200 km from HAARP. the vertical scale is logarithmic, and is in absolute units. Amplitudes of the maximum signal are printed at the various peaks.	10
6. Amplitude in mV/km of the Ex electric component corresponding to Figure 5.	10
7. Basic geometry of earth-ionosphere model showing HAARP RF beam and horizontal magnetic dipole at the base of the ionosphere.	12
8. Equivalent set of image line dipoles used to compute the antenna pattern.	13
9. Comparison of measured ELF amplitudes at Gakona and Sutton (solid dots) with model amplitudes. The amplitude scale at the left is in dBH, and at the right in pT.	14
10. Color coded amplitude distribution of ELF radiation from HAARP at 1 kHz. The intensity is normalized to 0 dB at HAARP. Contours of constant amplitude are drawn at 3 dB intervals.	15
11. Amplitude distribution of ELF radiation from HAARP at 4 Hz.	15
12. Ellipticity parameters for two intervals of strong LH ( $e \sim -0.5$ ) elliptical polarization at Slide Mountain, 8 Sep 2000.	16
13. Ellipticity parameters for two intervals of strong RH ( $e \sim +0.6$ ) RH elliptical polarization at Sutton, 14 Sep 2000.	16
14. This plot shows the variation of ionospheric and wave properties with altitude that are important in the study of ducted electromagnetic waves. The left panel shows the electric field perturbations of the waves; the center panel shows the variation of Alfvén speed of the waves; the right panel shows the variation of Hall and Pedersen conductivities. This diagram is taken from Fujita (1978) and represents nominal daytime conditions.	18
15. Field-aligned current, electron velocity, ion velocity, and electron number density as a result of the two-dimensional three-fluid ionospheric simulation model.	24

16.	Power vs. range of radar scatter from August 7, 2000 between 0000 and 0400 UT.	28
17.	Geographic projection of scattered power at 0130 UT on August 7, 2000	29

## Tables

1.	Basic characteristics of Gakona and Poker Flat systems as follows:	3
a.	Analog system	3
b.	Data acquisition system	3
c.	Software modules	4
2.	Experiment Log	20

# ***Diagnostics and Modeling of the Auroral Ionosphere under the Influence of the Gakona HF Transmitter***

## **1. Element 1: ELF/VLF Wave Measurement and Interpretation Program**

### **1.1 Summary**

The overall objective of Element 1 is to establish the characteristics of the ionospheric source region responsible for the ELF/VLF waves generated by modulation of HAARP HF emissions. To accomplish this objective we established two sub-objectives. The first was to establish ELF monitoring capabilities over the passband of interest to HAARP studies, generally 5-10,000 Hz, at two base or reference sites for routine experimenter use during and between campaigns. The second was to measure the ELF radiation pattern. The first sub-objective and the observational and preliminary interpretation components of the second sub-objective were met during the 18 month period covered by this Interim Report.

### **1.2 Introduction**

We describe first the ELF facilities instruments to monitor the effects of HF modulation of the Polar Electrojet (PEJ) at ELF and VLF frequencies. This is followed by a description of the Fall 2000 campaign to measure the radiation pattern, and results of the preliminary analysis of the observations.

### **1.3 The Gakona and Poker Flat ELF Systems**

#### **1.3.1 Methods, Assumptions and Procedures**

The measurements are made at two locations. One site, close (~10 km) to HAARP, is located north of Gakona and used to monitor the near field ELF/VLF emissions. A second site is located at Poker Flat at a distance of 350 km from HAARP. These systems were developed to give HAARP experimenters easily accessible ELF monitoring capabilities and for baseline signal levels for comparison with other remote measurements. The two systems are configured to be as close to identical as possible. The sensors at each site are electrostatically shielded induction coils optimized for operation in the frequency band 3-12,000 Hz. They are installed horizontally along North/South and East/West axes and measure the orthogonal horizontal components of the magnetic field. Sensor outputs are delivered via optical fiber to a real-time data acquisition and analysis system. Figure 1 shows the sensors and instrument trailer at Gakona. The real time computer systems convert the signals to digital form at 27.8 kHz using GPS synchronization, and perform various signal conditioning and filtering operations, and compute a variety of diagnostic information. These include synchronous detection of HAARP modulation frequencies, waveform stacking, and dynamic frequency-time spectra and amplitude distributions. The system can be remotely configured and administered over the Internet. The basic characteristics of the Gakona and Poker Flat systems are given in Table 1.

**Figure 1. Sensor box sensors and instrument trailer at Gakona ELF site.**

*Table 1a. Analog System (Basic characteristics of Gakona and Poker Flat systems)*

**Analog System**

Component	Description
• Sensors	EMI BF-10 Induction Coils 3-12000 Hz; sensitivity 1 pT/Hz <sup>1/2</sup>
• Receiver Hardware	Fiber optic connectors; 20-bit 48 kHz DSP; 60 Hz rejection comb filter, 16-bit, 44.1 kHz
• Time Standard	Spectrum Time Machine GPS

*Table 1b. Data Acquisition System (Basic characteristics of Gakona and Poker Flat systems)*

**Data Acquisition System**

Component	Description
• Digital Platform	PC, 350 MHz Intel Pentium II
• OS	Microsoft Windows NT 4.0 Server
• A/D Subsystem	Data Translation DT-3001 12-bit ADC/DAC/CTR; external triggering from GPS source
• Network	Ethernet, TCP-UDP/IP
• Software Architecture	Client-server; real-time data server feeding client analysis modules
• Data Base Format	NetCDF, HAARP conventions
• Remote Control	Various; principally NetMeeting and pcAnywhere

*Table 1c. Software Modules (Basic characteristics of Gakona and Poker Flat systems)*

**Software Modules**

Module	Function	Status
• Data Server	Sample data at 27.8 kHz, low pass filter and subsample into 4 user selectable filter banks	Operational
• Synchronous Detection	Detect and log amplitude and phase narrow band signals at up to 16 user specified signal and 8 noise frequencies 3-10000 Hz with absolute phase stability < 1 us; arbitrarily long integration intervals; linear and non-linear detection options	Operational
• Spectra	Compute and log dynamic spectra 3-200 Hz	Operational
• Time Series	Log sampled data	Operational
• Q-Burst	Detect and log ELF transients	Operational
• Amplitude Probability Distributions	Assemble and log amplitude probability distributions; used as input to non-linear option of synchronous detection module	Under development
• Stack	Assemble and log stacked periodic waveforms of arbitrary period	Operational
• Multisite	Differential measurements across long baselines.	Under development

In establishing these systems, numerous engineering difficulties were isolated and removed. An absolute calibration procedure was developed to provide end-to-end amplitude and phase response of the ELF receiver systems over the passband 3-Hz to 10 kHz. A short description of the overall characteristics of the ELF/VLF systems was created for inclusion into the HAARP brochure prepared by John Rasmussen.

An example of results obtained the Gakona ELF system during the Fall 2000 campaigns is shown in Figure 2.

### 1.3.2 Antenna Pattern Measurements

#### 1.3.2.1 Preliminary Site Survey

Following the 1998 Santa Fe meeting Gene Wescott visited Zonge Engineering in Tucson AZ to discuss changes in hardware to the GDP 32 II data recorder system and software needed to record HAARP transmissions for the proposed antenna pattern survey, and to be able to use the equipment for controlled source magneto telluric (CSAMT) resistivity vs. depth exploration with HAARP as the controlled source. After making some engineering modifications to the data recorder system, the equipment and software were delivered in time for field work during the HAARP June/July 1999 campaign.

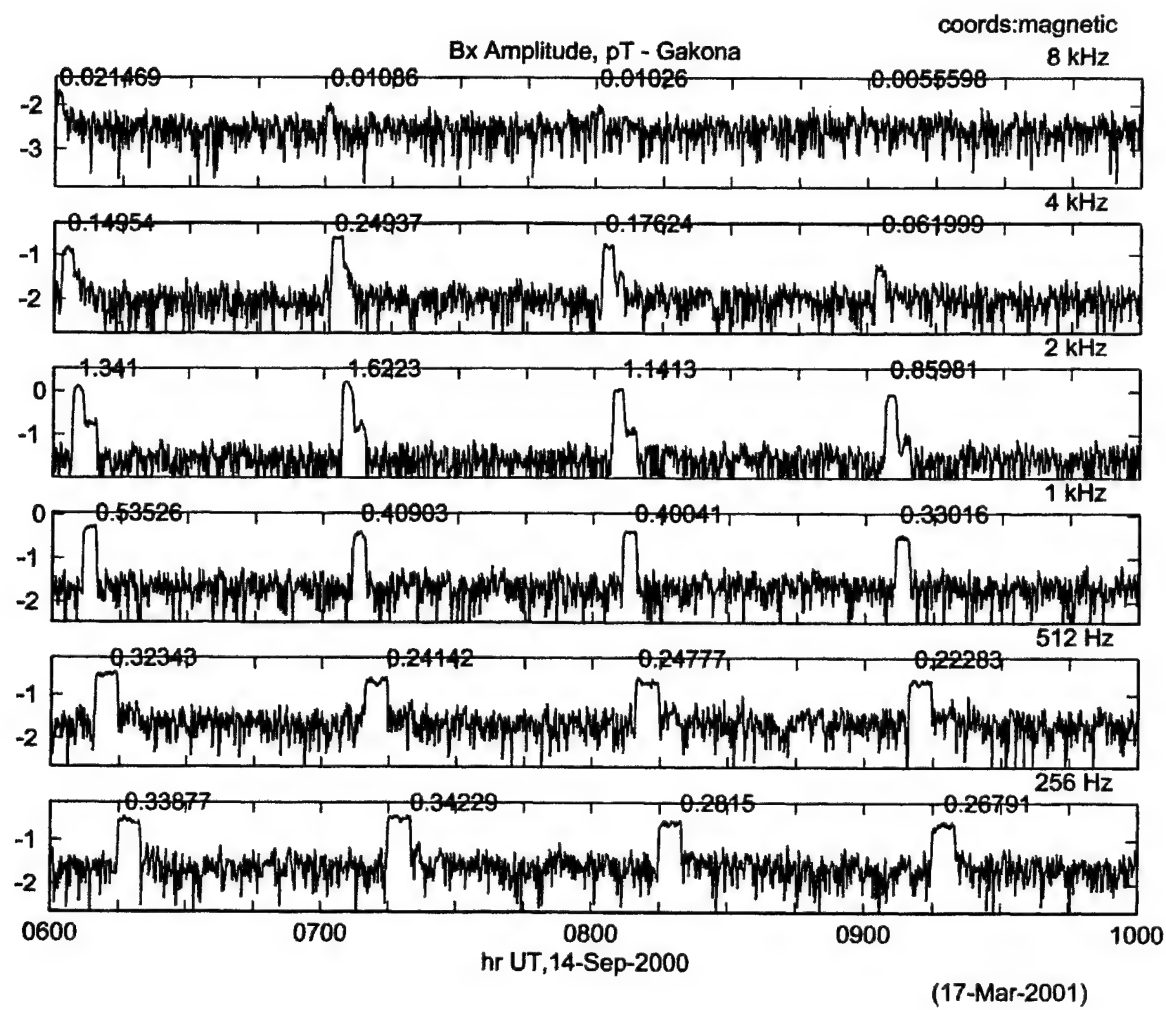


Figure 2. Synchronously detected horizontal magnetic field, Bx, signals between 256 and 4000 Hz from the Fall 2000 campaign.

First tests were made in conjunction with HAARP transmissions. Observations were made from the site near a capped wildcat well, Tazlina # 1, located about 75.6 km from HAARP on the Lake Louise Road, for which logs exist. The resistivity logs start at a depth of 340 m, where the resistivity is about 5 Ohm-m. The site is about 6 miles away from any 60Hz power lines, and proved to be a very quiet location. After several nights of unsuccessful tests, on the night of July 2 HAARP was modulating the beam at frequencies at powers of 2 from 4 Hz to 8192 Hz and very strong signals were received.

The HAARP signal apparent resistivity vs. frequency was converted to resistivity vs. depth using the Bostick algorithm as shown in Figure 3. Some minor smoothing was required for a few points. The results from the Ey/Hx apparent resistivity are shown in the figure. The resistivity log from Tazlina #1 starts at a depth of 340 m, because the well was cased to that depth, so we cannot compare the log and the CSAMT data directly. The logged resistivity starting at 340 m is almost constant 5 ohm-m in reasonable agreement with our deepest values. The obvious sediments near the surface at the site are well rounded river sediments and silts compatible with the 20 to 25 ohm-m values measured with the CSAMT closest to the surface.

During the September/October 1999 HAARP campaigns, preliminary measurements were made at several sites to test our equipment and analysis techniques that were subsequently used for the antenna pattern survey and characterization. We successfully measured two components of H and the corresponding E fields at a site 50 km from HAARP at frequencies: 16, 32, 64, 128, 256, and 512 Hz. The analysis of the data used a modified version of software used in the synchronous detection modules of the Gakona and Poker Flat systems. Following this successful test, plans were made to obtain three specially modified data loggers for the full antenna pattern measurement campaign in the spring.

### **1.3.2.2 *Sites for Antenna Pattern Measurements***

In June 1998 a preliminary survey was conducted of sites at 50, 100, and 200 km distance from HAARP to determine the suitability of 12 sites, as the minimum we would need in the survey. At each site we used the natural electromagnetic noise from the ionosphere in the audio magneto telluric (AMT) method to determine the background noise spectrum and the ground resistivity vs. frequency. We also measured 60 Hz power line and harmonics noise for interference. Likely sites at 150 km distance were also located, but due to shortage of time were not measured for magneto telluric resistivity.

Following the summer 1999 preliminary field survey, we expanded the number of remote measurements systems to include three leased Zonge systems in addition to the existing one, for a total of four. This would permit making measurements from four sites simultaneously. With this scheme it was decided to use the four systems distributed approximately in four quarters on circles centered on HAARP at distances of 50, 100, 150 and 200 km. These sites had to be located on drivable roads. Maps selected a suite of likely sites, and the University Office of Land Management sought permission for temporary use of the land to make the measurements. The land was owned by various owners or managers: U.S. Forest Service, U.S. Bureau of Land Management, State of Alaska, and Ahtna Native Corporation, and various native village corporations. Figure 4 shows the sixteen remote sites actually used in the HAARP survey, plus the site at Gakona. The natural source AMT measurements could be used to compare with the results calculated from the ratios of the electric and magnetic components of the HAARP signals.

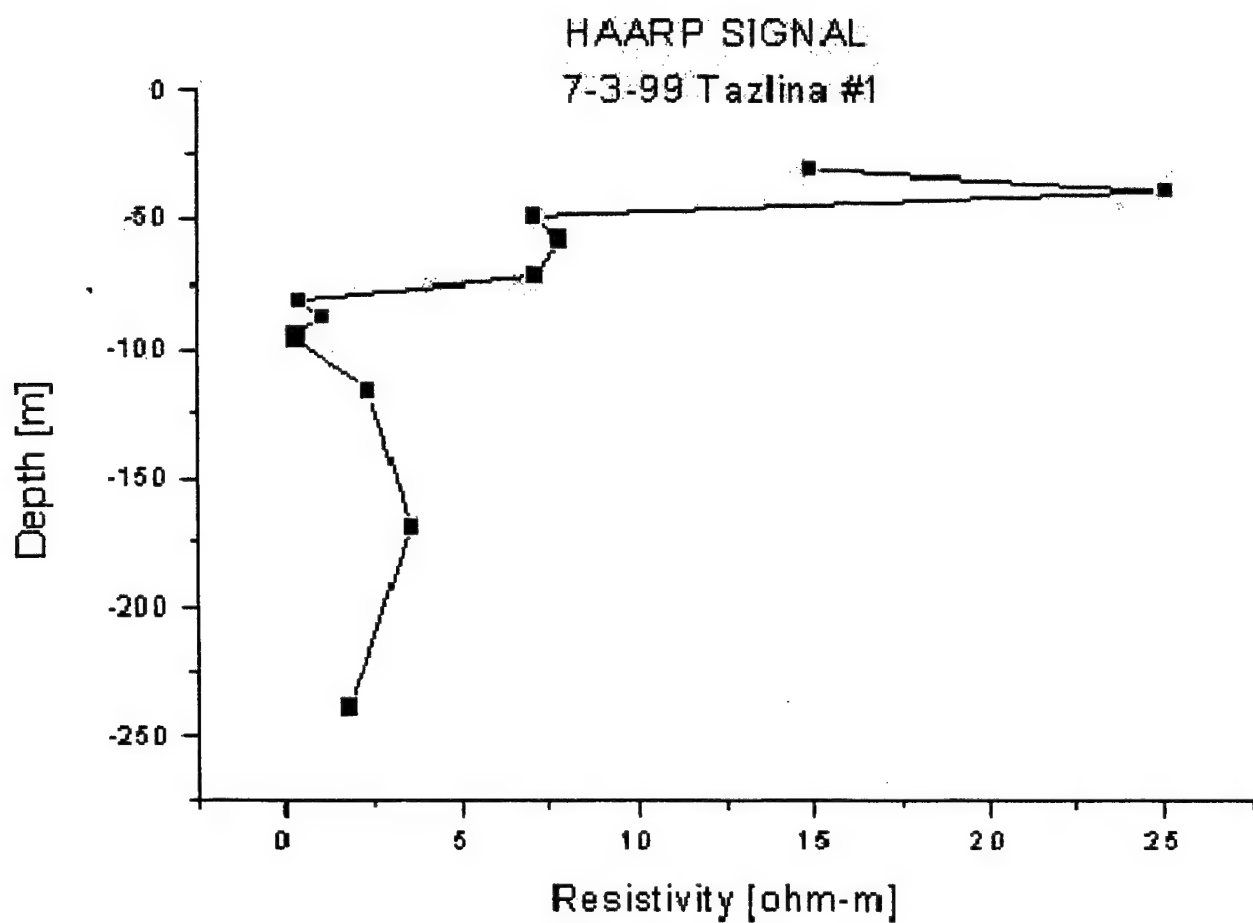


Figure 3. Resistivity vs. depth calculated using the Bostick algorithm derived from the modulated HAARP signal.

## HAARP 2000 Fall Campaign ELF Site Locations

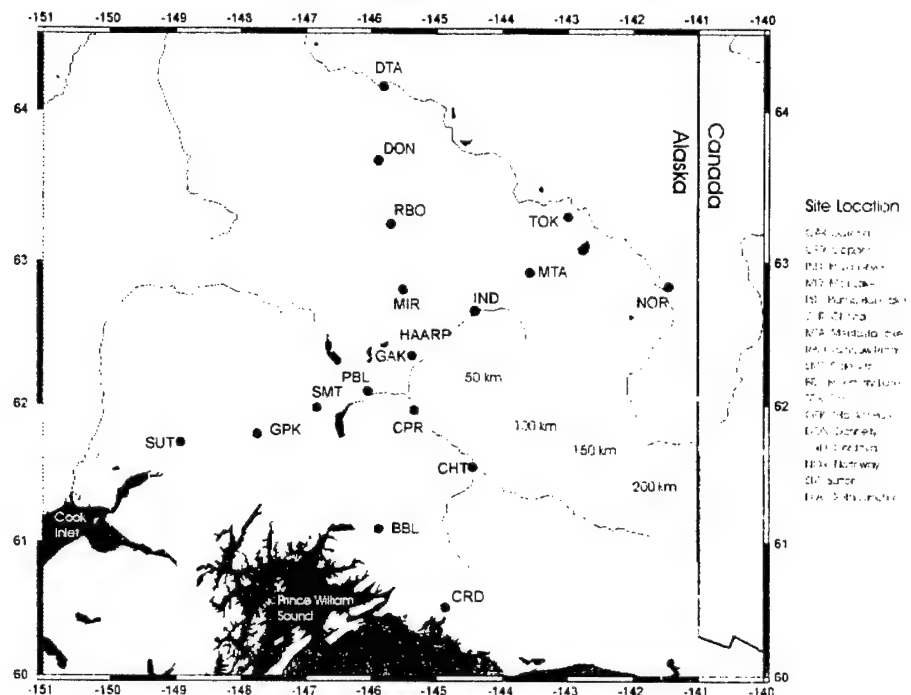


Figure 4. Remote field sites used for antenna pattern measurements, plus the Gakona reference site and the HAARP location. The HAARP location is indicated in gold. The legend at the right refers the site designations to their names.

In order to make the necessary two-component B field measurements to determine the HAARP antenna pattern, we first experimented with a Zonge Engineering data recording system and coils purchased for the project. The GDP-32 II is a multi-channel receiver designed to acquire virtually any type of electromagnetic or electrical data within the DC to 8 kHz bandwidth. It is waterproof and portable. The time base is an oven controlled oscillator with  $5 \times 10^{-10}$  per 24 hours aging rate. The system was equipped with GPS-disciplining for greater timing control. The two Zonge coils have a flat response of 100 mV/nT over the frequency range of interest.

## 1.4 Results and Discussion

### 1.4.1 Fall 2000 Campaign

Permission for an extended field campaign in September 2000 was obtained from all the pertinent land owners, and a contract was let for the lease of three Zonge GDP 32-II data loggers and magnetometer coils. All the antenna pattern field measurements were carried out by four crews operating from four rented motorhomes to provide accommodations at the remote field sites. They were equipped with generators for providing 60 Hz power for recharging batteries and transferring the data to digital tape. In order to reach the 200 km distance site about 40 miles from Cordova, a charter aircraft was flown from Valdez.

The field campaign began on September 5, 2000 with measurements of both E and H components at 4 sites each 50 km distant from HAARP. Observations at each site continued on successive nights until the HAARP magnetometer coils at Gulkana indicated strong signals. Excellent data were obtained on the UT nights of September 7 at 50 km, September 8 at 100 km, September 12 at 150 km and 14 September at 200 km distances. (UT). The very best night of ELF/VLF activity occurred on the night of September 14. All the field data were copied from the digital tapes to the DVD format, with a spare set for backup. The data from the four nights at the four distances, have been spectrally analyzed and it is clear that excellent data were obtained at all distances out to 200 km from HAARP. The frequency range with good data includes 4, 8, 16, 32, 64, 128, 256, 512, 1000, 2000 and 4000 Hz

All the field data were copied from the digital tapes to the DVD format, with a spare set for backup. Sample data from each night, at each site were spectrally analyzed to determine the quality of the data obtained from each of the sixteen sites. The frequency range with good data includes 4, 8, 16, 32, 64, 128, 256, 512, 1000, 2000, and 4000 Hz at all distances out to 200 km. The total sampled data for the campaign comprised approximately 40 GB.

### 1.4.2 Data Analysis

Several kinds of data analyses were performed on the observations.

#### 1.4.2.1 Amplitude and Phase of HAARP-Generated Modulation Signals

The data from each site comprised signals sampled at 4096/sec. Amplitude calibrations for each of the electric and magnetic channels were applied to the data to produce absolute signal levels. From these sampled data the amplitude and phase were computed for each of the individual frequencies 4, 8, 16, 32, 64, 126, 256, 1000, and 2000 Hz. Figure 5 shows sample results 256-4000 Hz for the By channel obtained from Cordova on 14 September 2000. Figure 6 shows the corresponding results for the Ex channel.

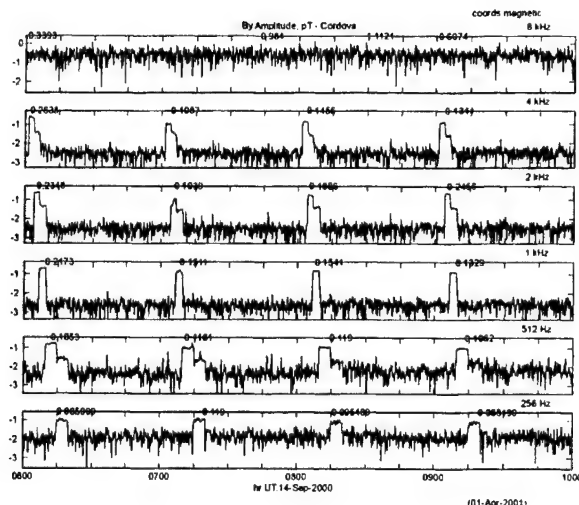


Figure 5. Amplitude in pT of the By magnetic component of synchronously detected HAARP signals obtained 14 Sep 2000 from Cordova, 200 km from HAARP. The vertical scale is logarithmic, and is in absolute units. Amplitudes of the maximum signal are printed at the various peaks.

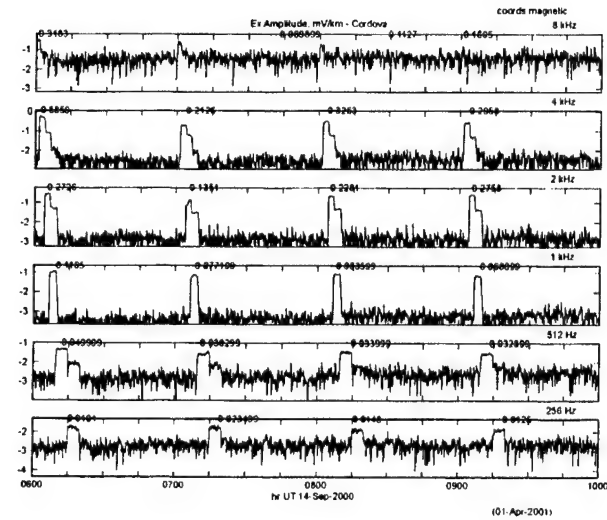


Figure 6. Amplitude in mV/km of the Ex electric component corresponding to Figure 5.

#### 1.4.2.2 Preliminary Interpretation

Amplitude and phase calculations were performed on all data. The results were analyzed by Peter Bannister to produce a preliminary model of the radiation pattern based on the observed amplitudes and phases at the measurement sites.

The basic ionospheric model is shown in Figure 7. In this preliminary model the ionosphere is assumed to be a homogenous slab of constant conductivity  $3 \times 10^{-5}$  S/m, with a base at altitude  $h$ . The perturbed electrojet is assumed to create a horizontal magnetic dipole with moment  $m$ .

The adjustable parameters in this model are the ionospheric conductivity, the dipole magnitude  $m$ , its height  $h$  and its orientation. The equivalent image line dipole model is shown in Figure 8. By adjusting the model parameters, a good fit was obtained to the simultaneous measurements at each of the remote sites. Figure 9 shows an example of the quality of the fit obtained between the observations made at the Gakona base site and Sutton, 210 km west of HAARP and the model. The data indicate the effective height of the magnetic dipole was at 91.5 km, and had a moment of  $3.1 \times 10^9$  A-m<sup>2</sup>. The orientation was magnetic north-south. For this particular run the magnetic amplitudes were maximum at 2 kHz at Gakona, at a value of ~3 pT. The corresponding value at Sutton was ~0.5 pT. Similar analyses were performed for each of the other stations for each of the nights on which good signals were obtained. The resulting ionospheric dipole model yields intensity maps as functions of frequency and position for distances to ~300 km from HAARP. Figures 10 and 11 show intensity maps for 4 Hz and 1 kHz obtained from the observations. They are normalized to 0 dB at HAARP. Of interest in these maps is the existence of nulls at magnetic north-south distances from HAARP of ~100 km.

#### 1.4.2.3 *Polarization*

The elliptical polarization parameters were extracted from the amplitudes and phases of the orthogonal horizontal components of the magnetic and electric fields. These parameters are useful in separating time varying effects of the anisotropic ionosphere from effects induced by anisotropies in the local ground conductivity. Examples of polarization parameters derived during two nights exhibiting both left-hand (LH) and right-hand (RH) polarizations, respectively, are shown in Figures 12 and 13.

### 1.5 Conclusions

A preliminary report with the results shown here was presented at the RFII Meeting in Santa Fe in May, 2001. These results are based on modeling the amplitudes as measured at each of the various sites. A more complete analysis that makes use of the vector measurements and polarization properties has been initiated. A formal and complete description of these observations and their interpretation will be prepared for publication in Radio Science.

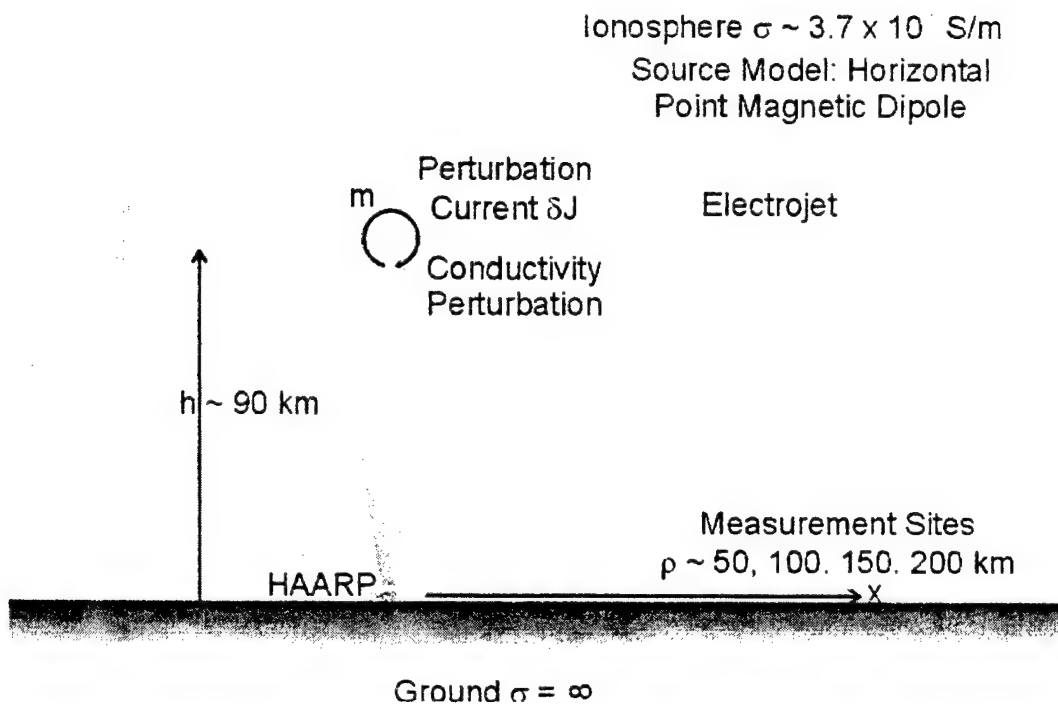


Figure 7. Basic geometry of earth-ionosphere model showing HAARP RF beam and horizontal magnetic dipole at the base of the ionosphere.

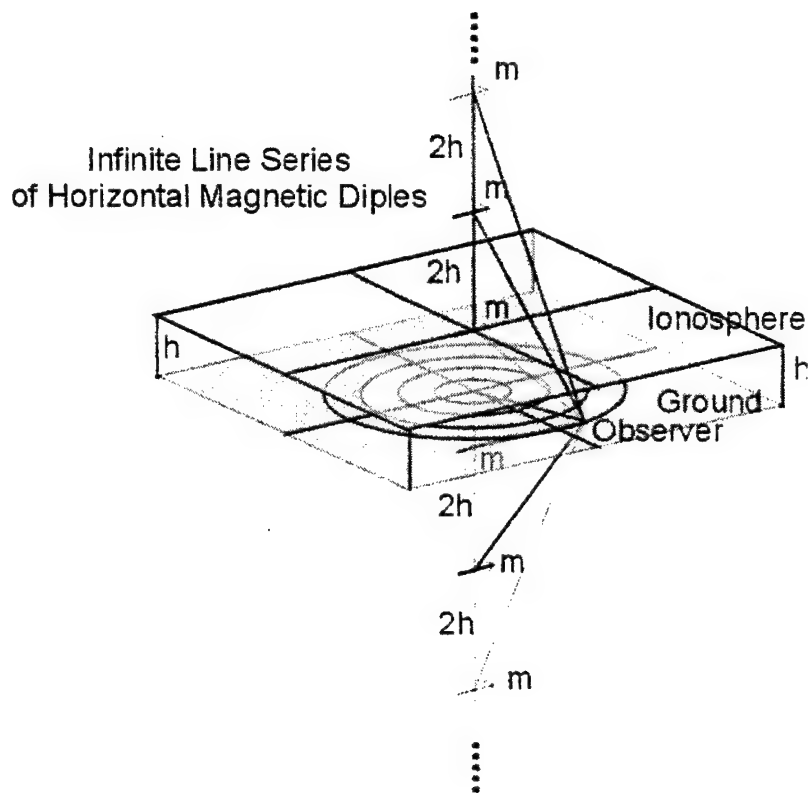


Figure 8. Equivalent set of image line dipoles used to compute the antenna pattern.

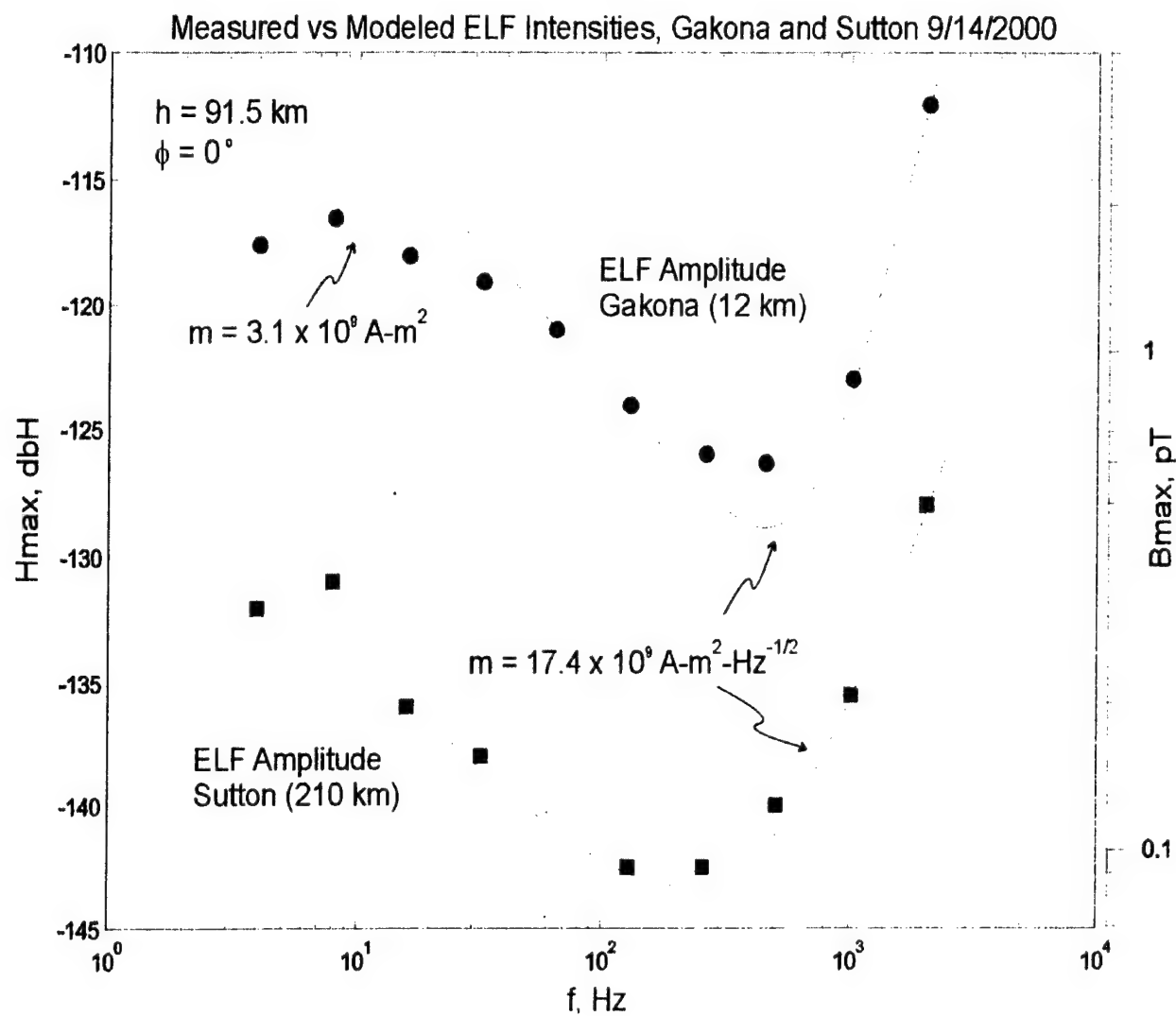


Figure 9. Comparison of measured ELF amplitudes at Gakona and Sutton (solid dots) with model amplitudes. The amplitude scale at the left is in dBH, and at the right pT.

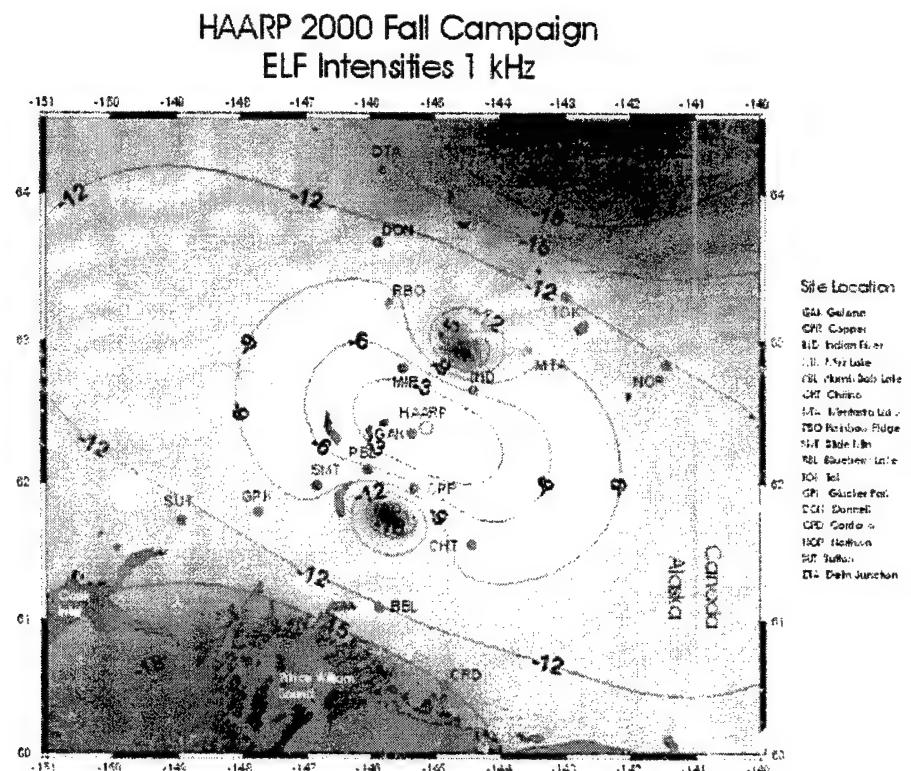


Figure 10. Gray-scale coded amplitude distribution of ELF radiation from HAARP at 1 kHz. The intensity is normalized to 0 dB at HAARP. Contours of constant amplitude are drawn at 3 dB intervals.

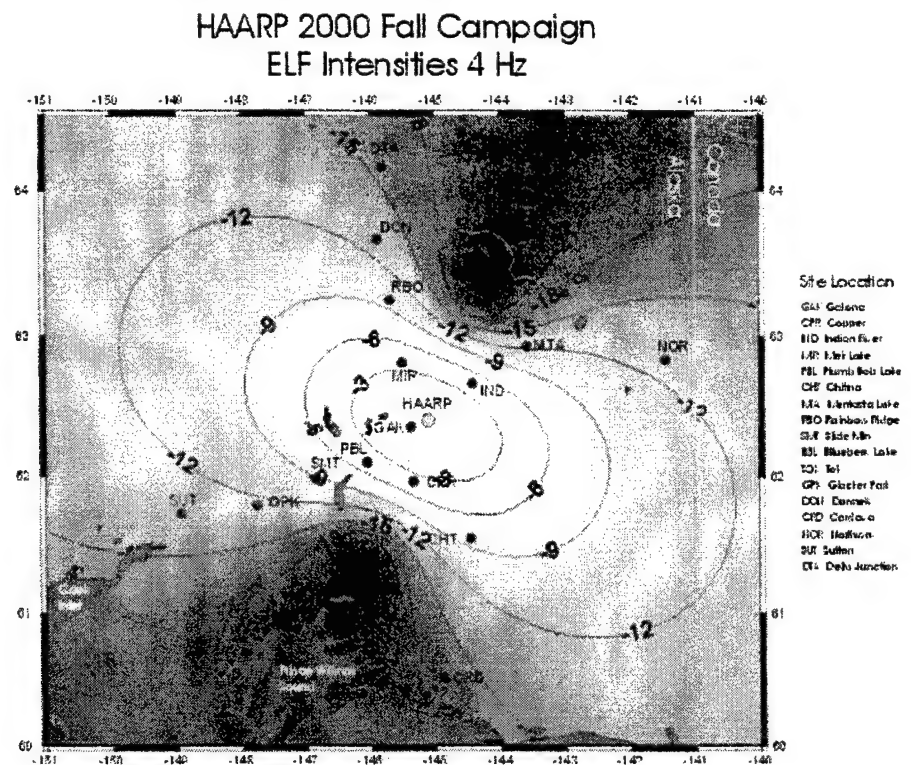


Figure 11. Amplitude distribution of ELF radiation from HAARP at 4 Hz.

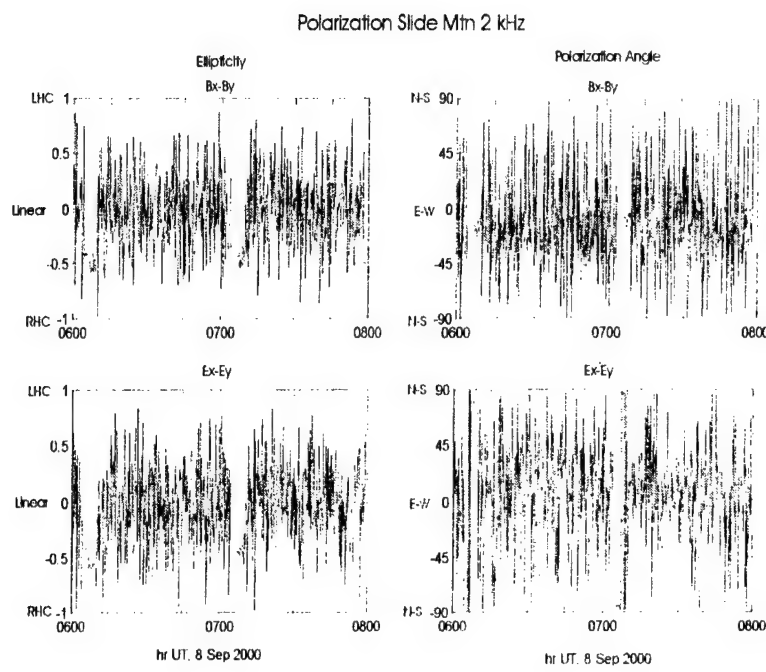


Figure 12. Ellipticity parameters for two intervals of strong LH ( $e \sim -0.5$ ) elliptical polarization at Slide Mountain, 8 Sep 2000.

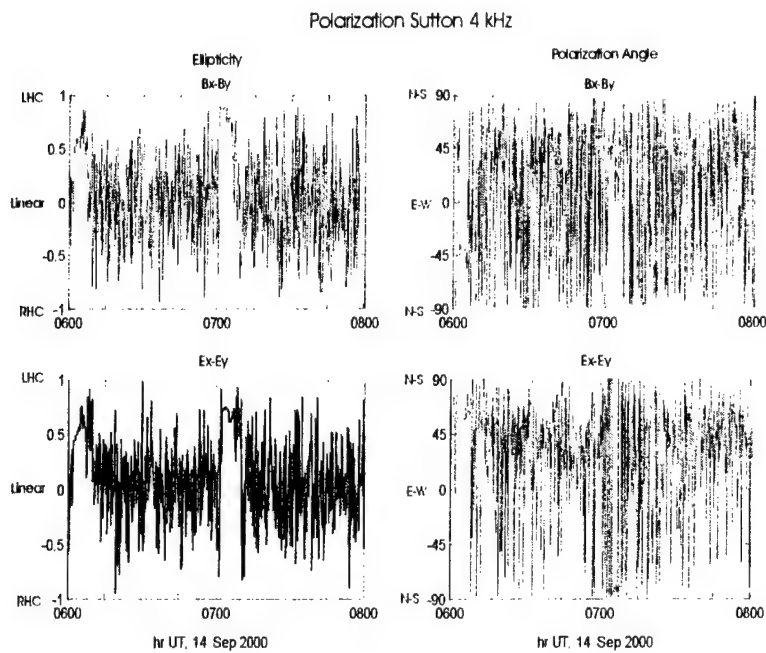


Figure 13. Ellipticity parameters for two intervals of strong RH ( $e \sim +0.6$ ) RH elliptical polarization at Sutton, 14 Sep 2000.

## 2. Element 2: ULF Wave Measurement Program

### 2.1 Summary

The purpose of our experiment is to attempt to stimulate hydromagnetic waves in the ionospheric wave-guide using the HAARP heater. A wave-guide exists in the earth's ionosphere due to the maximum charge density located in the F-Region. This 'duct' allows ULF pulsations in the 0.1 – 5 Hz band to propagate across large horizontal distances from the source location.

Ionospheric wave-guide theory tells us that two wave modes can exist in the duct, coupled by the Hall conductivity. We have hypothesized that modulated heating of the ionosphere can cause a variation in the Hall current that will serve as a source of ULF waves. We have employed two induction magnetometers, operated by the Geophysical Institute at College and Kaktovic, Alaska, to detect the ULF signals that are produced in the duct.

The experiment has been run three times, however we have not yet been successful. While we have evidence that the duct was present during our earlier runs and that our instruments are sensitive enough to detect any signals generated, we do not know the topology of the currents generated by the heater. If the current patterns are complex there may not be a significant amount of radiation produced. A better analysis and understanding of the heated region along with a more detailed theoretical experimental basis is needed for further trials.

### 2.2 Introduction

#### 2.2.1 Background

##### 2.2.1.1 The ionospheric wave-guide

As a consequence of the variation in electron and ion densities in the ionosphere, the index of refraction for low-frequency electromagnetic waves that can propagate in the ionospheric plasma also varies. The phase speed of these waves, termed the Alfvén speed, is proportional to the inverse-square root of the charge density and is shown in the middle panel of Figure 14 for nominal ionospheric conditions.

The presence of a minimum in the phase speed at approximately 300km altitude in the F region of the ionosphere indicates that electromagnetic waves may propagate horizontally near the minimum in the Alfvén speed. This region is termed the "ionospheric wave guide" or "duct".

Many investigators (e.g. Greifinger and Greifinger, 1968, 1973) have carried out theoretical analyses of this situation and, indeed, there are two electromagnetic wave modes that can propagate in the wave-guide. The wave amplitudes of the two modes are shown in the left panel of Figure 14. The dominant mode, labeled  $\delta E_y$ , is the mode that propagates horizontally along the duct. The second mode, labeled  $\delta E_x$ , is constrained to propagate along the (vertical) magnetic field direction. Analysis shows that the two wave fields are coupled by currents that depend upon the Hall conductivity. Observations that provide evidence of ducting of naturally occurring electromagnetic waves have been made for many years and will be described below.

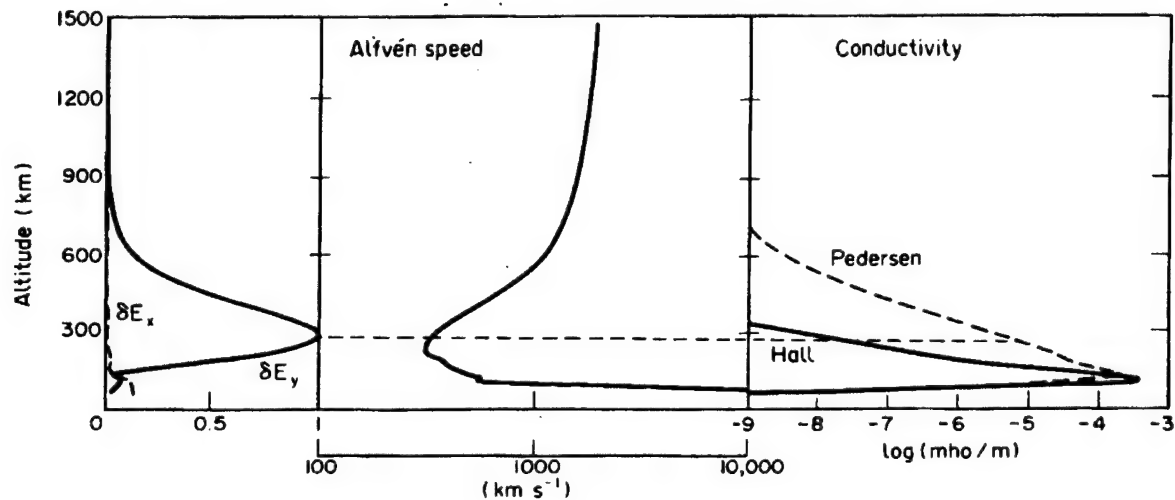


Figure 14. This plot shows the variation of ionospheric and wave properties with altitude that are important in the study of ducted electromagnetic waves. The left panel shows the electric field perturbations of the waves; the center panel shows the variation of Alfvén speed of the waves; the right panel shows the variation of Hall and Pedersen conductivities. This diagram is taken from Fujita (1978) and represents nominal daytime conditions.

As the right panel shows, the Hall conductivity is largest at the bottom of the wave-guide. Although the maximum normally lies between 100km and 125km the conductivity is significant over an interval from 80km to 150km. This is the key to our proposal. We hope to heat the ionosphere in the region where the Hall conductivity is large so that the ambient electric fields can drive currents large enough to radiate electromagnetic energy into the duct, coupling the locally stimulated wave to the propagating mode.

While the theory of propagation in the ionospheric wave-guide is well established, some of the predictions of the formulations have never been verified. Among these is the presence of a low-frequency duct cut-off similar to the cut-off characteristics of electromagnetic wave-guides. A second prediction of the theory is an attenuation rate that is expected to be on the order of a few dB per 1000 km. However, the predictions vary and have never been measured.

### **2.2.1.2 Ducting of natural ULF emissions**

For several decades electromagnetic waves in the Ultra-Low Frequency (ULF) band (dc to 3hz) have been detected by magnetometers at the earth's surface (see von Stetten, 1999). The waves have been identified as electromagnetic ion-cyclotron waves that are the result of instabilities in the distant equatorial magnetosphere. Principally generated in the equatorial regions near  $L=4$  on the afternoon side, these pulsations propagate along the magnetic field to the ionosphere. Once incident on the ionosphere they have been shown to be ducted to regions far from the source field line.

When the polarization state of the various classes of  $Pc1$  signals are analyzed a mixture of right-hand and left-hand polarization is observed. Since the left-hand mode cannot propagate in the ionospheric wave-guide while the right-hand polarized wave can, the presence of right-hand signals indicates the pulsation has traveled to the observation point via the ionospheric wave-guide. Also, the attenuation rate of waves propagating along the duct has not been measured.

## **2.3 Methods, Assumptions and Procedures**

The experiment was set up so that the HAARP heater would heat the D-region of the ionosphere with a carrier frequency of 3.3 MHz while modulating the amplitude of the radiation as a sine wave at frequencies in the ULF range of 0.1 - 1.2 Hz.

For the experiment we chose four different beam modulation frequencies: 0.3, 0.5, 0.7, and 0.9 Hz, and we heated in the X-mode at each modulation frequency for 15 minutes. Below is the time log of our experiment:

Table 2: Experiment Log

Time (UTC)	Frequency (Hz)
02:30:00	0.3
02:44:30	off
02:45:00	0.5
02:59:30	off
03:00:00	0.7
03:14:30	off
03:15:00	0.9
03:29:30	off

## 2.4 Results and Discussion

Using synchronous detection techniques we scanned the induction magnetometer data from College and Kaktovic, Alaska during the periods that the HAARP heater was operating in the ULF modulation modes we requested. We did not detect signals above our threshold of 2 pT.

## 2.5 Conclusions

Although we have evidence that the ionospheric duct was “open” (natural ULF signals were observed during the experimental period) we did not observe any signals associated with the HAARP heating above our instrument threshold. We believe that this may be due to the configuration of currents that flow in the heated region. If the currents are not linear but rather coruscated then it may be that their effective dipole moment is small yielding small radiated field amplitudes. It is our intention to continue these experiments in the hope that we may find the ambient conditions that will allow for successful stimulation of ULF waves.

## 2.6 Scientists and engineers who contributed to the research reported in this document

Dr. John V. Olson, Geophysical Institute, University of Alaska

Mr. Keith Carney, Geophysical Institute, University of Alaska

## 3. Element 3: Auroral Ionosphere Modeling Program in Support of HAARP

### 3.1 Summary

This element of the HAARP project develops a simulation model for the plasma physical and electromagnetic effects of localized ionospheric heating with the purpose of predicting outcomes of heating experiments and to guide the design of new experiments. Modeled

properties are densities, velocities, and temperature of electrons and ions as well as electric and magnetic perturbations up to a frequency of about 1000 Hz.

During the past funding phases we have completed the two-dimensional model including a verification of results through comparison with various test cases. The development of the three-dimensional simulation model is underway and first test results have been obtained.

### 3.2 Introduction

A simulation of ionospheric heating and its plasma physical and electromagnetic effects can be of large importance to guide heating experiments. The simulation must include the relevant ionospheric physics which in particular includes: Ionization and recombination, ion-neutral friction, a form of Ohm's law which includes Hall physics and the electron pressure effects, and equations for electron and ion energies including heat conduction.

Such a model is able to realize physics down to the ion inertia scale of about 1 km (at the relevant ionospheric heights) and temporal scales up to about 1000 Hz. Considering the geometry of the heating processes a three-dimensional model is required for many applications.

With the simulation model it will be possible to study the ionospheric modifications for instance due to changes of the ionospheric conductances. The generation of hydro-magnetic plasma waves as a result of the heating and consequences for corresponding observations can be analyzed and predicted.

The completed three-dimensional model may serve to guide the design of heating experiments.

### 3.3 Methods, Assumptions and Procedures

The simulation model is aimed at meso-scale ionospheric physics (one km to a few hundred km). This is accomplished by using a three-fluid approximation that covers electron, ion, and neutral dynamics. For each species the simulation model integrates the continuity equation, the momentum equation, and the energy equation. To facilitate the desired scales electron inertial effects are neglected (20 m scale). Otherwise the complete fluid moments are solved in a time-dependent fashion.

The continuity equations contain effects of ionization and recombination in a parameterized form. The momentum equations consider plasma neutral friction, and Ohm's law includes electron pressure gradients and the Hall term. Finally the energy equations include heat conduction and a defined localized heat source in addition to heating by precipitation and frictional (Joule heating) causes.

The ionization rate, the recombination frequency, and the electron heating rate associated with ionization are parameterized by using input from kinetic ionospheric transport computation. The electron heat conduction coefficient and the effective electron-neutral, ion-neutral, and electron-ion collision frequencies are from the National Center for Atmospheric Research (NCAR) thermosphere ionosphere mesosphere electrodynamics general circulation model (TIME-GCM).

The model is based on prior models which we ran for MHD cases and two fluid systems. It uses a Dufort-Frankel integration scheme which is of sufficient accuracy and sufficiently fast to treat the described problem in three dimensions. The models are initially developed for vector supercomputers and should be parallelized in second phase to allow for sufficiently fast performance.

The simulation region extends from 900 km (lower E region) to 1100 km altitude with the main magnetic field in the vertical direction. The neutral fluid is initially in hydrostatic equilibrium with a temperature  $T_n$  and density  $n_n$  chosen for solar minimum and solar maximum conditions from the Mass Spectrometer Incoherent Scatter (MSIS) model.

Different from global thermospheric simulation models, all physics which play a role on the considered spatial and temporal scales is included in the simulation model. This in particular applies to the ion inertia term with the result that typical fluid plasma waves such as Alfvén, whistler, fast and slow modes are included in our model. This allows for the propagation of guided ionospheric waves as well as for the formation of field-aligned currents through Alfvén waves.

### 3.4 Results and Discussion

The development of the two-dimensional simulation model has been completed. We have run the model for various applications with the purpose of verifying the simulation techniques and to identify new physical insight of meso-scale dynamics.

- Ionospheric heating through strong field-aligned currents

This work simulates a well documented event (EISCAT, Lanchester et al., 2000) of a discrete auroral arc and the associated ionization and heating. This event is characterized by a highly interesting sequence of electron density, electron temperature, and ion temperature evolution. Initially the ion temperature increased during a period of lowering electron density. During the subsequent decrease of the ion temperature, the electron temperature suddenly increased, however, several seconds before the electron density reached its minimum (and before the arc came into the field of view of EISCAT). This implies that heating through discrete precipitation cannot be the cause for the sudden electron temperature increase. Using the 2-D simulation code we have demonstrated that the sequence of events is nicely consistent with the passage of a strong field-aligned current layer through the field of view of EISCAT. The resulting electron heating in the strong field-aligned current and ion heating in the regions outside the current provide the correct temporal and height profiles for the electron and ion temperatures. This result provided very strong evidence for large field-aligned currents in the ionosphere and for their importance of heating the electrons in the F region ionosphere.

- We have used the simulation code to study the formation and the evolution of field-aligned current in the ionosphere. This particularly includes the closure of these currents through Pederson currents and the associated Hall currents. Figure 15 illustrates an example of the current system which is forming in the simulation. In this case two Alfvén waves are initiated at the magnetospheric boundary. These waves propagate into the ionosphere and carry two field-aligned current sheets (upward and downward current) down into the E-region. During the propagation the field-aligned currents are closed through polarization currents. After the reflection from the ionosphere the field-aligned currents are mostly closed through Pederson

currents. While the field-aligned currents are carried by electrons due to their small inertia, the closing currents are mostly carried by ions as illustrated in Figure 15. This, however, implies that the divergence of the electron flux is nonzero at the base of the field-aligned current layers (i.e., the region where the field-aligned currents close into Pederson currents). As a result the electron number density is strongly modified at the base of the field-aligned current with an increase for upward current layers and a depletion for downward current. Modifications of these currents as a result of precipitation and additional heating such as through the ionospheric heater have been studied. These simulations also demonstrate the formation of new field-aligned currents and Alfvén waves through heating in the presence of an electrojet current.

The results and many consistency tests have documented that the new simulation code provides reliable physical results. The first results which we obtained are new and highly interesting in the field of small and meso-scale ionospheric dynamics.

### **3.5 Conclusions**

1. We have completed the development of a two-dimensional meso-scale simulation model for the ionospheric parameters relevant for the HAARP facility. The new simulation code has been used to model a variety of ionospheric phenomena with focus on the formation and evolution of field-aligned currents, Alfvén wave propagation, electron and ion heating, and ionization through particle precipitation.
2. The simulation results demonstrate the formation and evolution of field-aligned currents and their closure. The closure of field-aligned currents implies density irregularities at the base of field-aligned current layers. Field-aligned currents can be imposed as a boundary condition at the magnetospheric boundary or can form in the presence of localized heating and precipitation.
3. The applications demonstrate the value of the new model to predict ionospheric dynamics. To our knowledge the simulation is the first time-dependent code that can resolve the typical fluid plasma waves in the ionosphere for the considered spatial and temporal scales.
4. The two-dimensional simulation results have been very encouraging and the development of the three-dimensional code is close to completion. We expect this code to be of high value for the prediction and guidance of ionospheric heating experiments in different plasma environments.

### **3.6 Scientists and engineers who contributed to the research reported in this document.**

Antonius Otto  
Hua Zhu  
Vincent Dols

### **3.7 All previous and related contracts and previously produced publications or articles**

Zhu, H., A.Otto, D. Lummerzheim, M.H. Rees, and B.S. Lanchester, Ionosphere-magnetosphere simulation of small-scale structure and dynamics, *J. Geophys. Res.*, 105, 1795-1806, 2001.

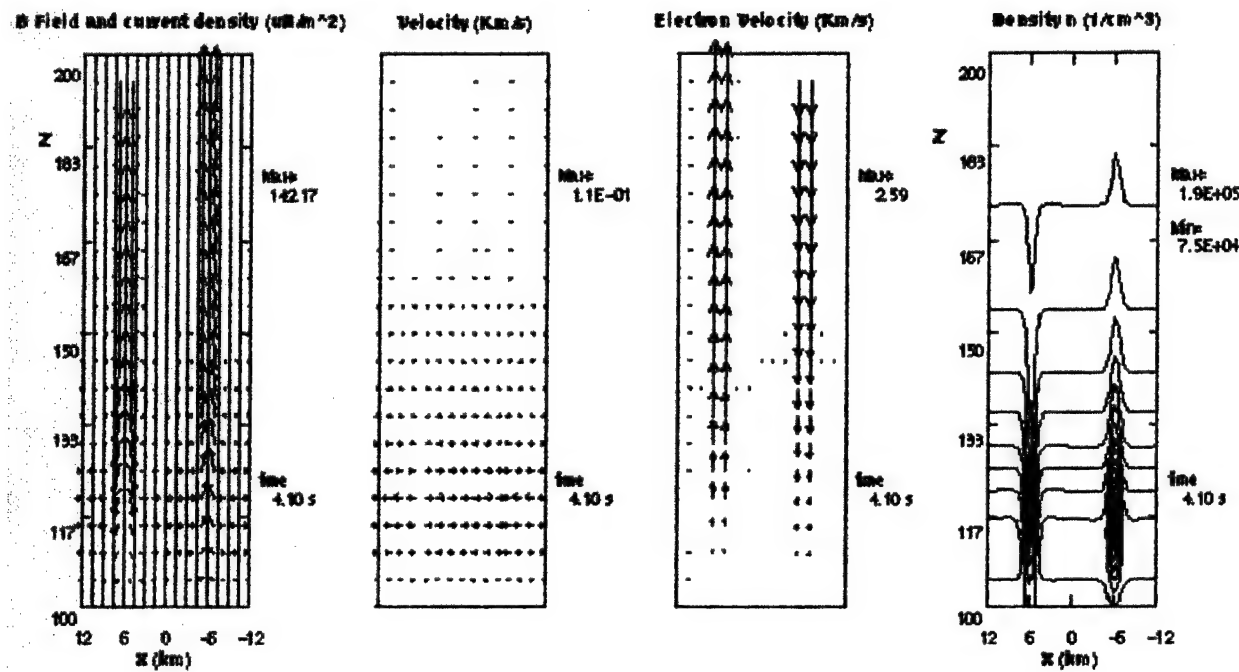


Figure 15. Field-aligned current, electron velocity, ion velocity, and electron number density as a result of the two-dimensional three-fluid ionospheric simulation model.

## 4. Element 4: SuperDARN Operations

### 4.1 Summary

Construction of the Kodiak SuperDARN radar was completed in January 2000 and the radar has operated continuously since that time. Each HAARP campaign since January 2000 has been supported with observations from the site. Electric field measurements have been available continuously and special operating modes have been implemented for specific experiments. Special operating modes were executed on nine days during this reporting period for a total of 39 hours of radar operation. The objective of the special operating modes was to examine the formation of ionospheric irregularities within the heated volume and to examine the relationship of the irregularities to other observations such as the generation of Stimulated Electromagnetic Emissions (SEE).

### 4.2 Introduction

The Kodiak SuperDARN radar is an HF radar that was built as part of the SuperDARN radar network. SuperDARN, the Super Dual Auroral Radar Network, consists of eight HF radars in the northern hemisphere and six radars in the southern hemisphere that were built to observe the signature of magnetospheric convection in the ionosphere. Radio signals are reflected from irregularities of the ionospheric plasma, which are generated naturally by plasma instabilities induced when an electric field is applied across plasma density gradients. At high altitudes, these plasma irregularities move with the bulk velocity of the plasma and, hence, the radio reflections can be used to trace the motions of the bulk plasma. The bulk motion follows the magnetospheric convection pattern and, by combining data from all the radars in the network, the convection pattern can be mapped and monitored as it changes in response to changing interplanetary conditions.

In addition to the global-scale convection pattern, the data are of sufficient resolution to determine the local electric field above the HAARP site. This electric field data can be used in conjunction with other observations and computer models to aid in understanding the generation of ELF from the heated volume.

Ionospheric heaters, such as HAARP, also induce plasma instabilities that produce irregularities from which radio signals scatter. While the instabilities are not the same ones that operate naturally, the resulting irregularities can be detected by an HF radar. Hence, the Kodiak SuperDARN radar acts as an excellent diagnostic of the ionospheric heating produced by HAARP.

### 4.3 Methods, Assumptions and Procedures

The Kodiak SuperDARN is a phased array radar operating in the HF frequency band (8 MHz to 20 MHz). The radar is steered electronically in 16 fixed azimuths separated by about  $3.25^\circ$  covering an azimuth sector of about  $52^\circ$  that is centered along an azimuth of  $30^\circ$  east of true north. The radar transmits a beam that is narrow in azimuth, about  $3^\circ$ , and broad in elevation angle, about  $15^\circ$  half power beam width. The peak elevation angle of the beam is in the range of about  $10^\circ$  to  $20^\circ$  above the horizon depending on frequency. Because the signal is in the HF

band, the signals are subject to refraction in the ionosphere and long distance propagation is possible. It is not uncommon for the radar to observe ionospheric scatter at ranges of more than 3000 km. The radar transmits short pulses and samples each beam direction into 75 range bins. The size of the range bins depends on the transmitted pulse length and usually is in the range from 15 km to 45 km. The radar dwells in each beam direction for a period of time, usually in the range from 1 second to 7 seconds, and integrates returns over the period. With these dwell times, the time to complete a sweep of all sixteen beams ranges from about 20 seconds to 2 minutes.

The signals are scattered from electron-density irregularities in the ionosphere; mostly from the F-region ionosphere. The scattering process is Bragg reflection, so the radar is sensitive to irregularities with spacing equal to one half of the radar wavelength. Hence, the radar senses the presence of decameter scale irregularities. Such irregularities are produced naturally through the gradient drift instability and are produced in the artificially heated volume through other instabilities. The scattering is a coherent process, so the scattering cross section is quite large and the radar needs to transmit only low power.

Special operating modes created for HAARP observations included high-range resolution, reduced scans, and repeated beams. The ionospheric volume above HAARP sits at about 650 km to 700 km range from Kodiak at an azimuth of about 30°. Scatter from the heated volume typically appears in the central eight radar beams. By scanning over only those central eight beams, the time to complete a scan is reduced and higher time resolution is achieved. The other way in which we have achieved high time resolution is to interleave a single beam between each beam of a scan. That is, the beam sequence would be beam 8, beam 4, beam 8, beam 5, beam 8, beam 6, beam 8, beam 7, etc. If the integration time for each beam is 3 seconds, then this mode would provide time resolution over the HAARP site of about 6 seconds.

#### 4.4 Results and Discussion

Radar scatter from the artificial irregularities has been observed during each of the scheduled experiments. Figure 16 shows a time series of the scatter observed on August 7, 2000. These data were taken during the HAARP summer school campaign in support of the experiment to generate SEE. The heater was cycled on and off and the irregularities appear and disappear with the heater cycle.

At the beginning of this interval, there was significant ionospheric absorption and no SEE were observed, and no ionospheric irregularities were observed. As the figure illustrates, the absorption abated as the experiment continued and irregularities were observed. SEE were observed at about the same time that the irregularities appeared.

Figure 17 shows some of the same data superimposed on a map of Alaska to illustrate the spatial extent of the scatter above the HAARP facility. Scatter is observed in 6 beams and in about 8 of the 15-km range gates covering a range of about 120 km. The region appears larger in azimuthal extent than in range extent because of the finite beam width of the antenna beam pattern. The observation is the convolution of the beam pattern with the area of irregularities.

#### 4.5 Conclusions

It can be concluded that the Kodiak SuperDARN radar is capable of observing scatter from ionospheric irregularities generated within the volume heated by the HAARP facility. The irregularities appear to be generated whenever ionospheric conditions allow the heater signal to reach

the F-region ionosphere. The scattering cross section of the heater-induced irregularities is generally large, allowing for short integration times. In recent experiments, the radar integration time has been as low as 1-second per beam and produced adequate signal to noise ratio to observe the heater induced irregularities. The induced irregularities appear to have a finite decay time and do not disappear until some period of time after the heater is turned off. The decay time appears to be lengthened when there is a significant ambient electric field.

#### **4.6 Recommendations**

It is recommended that experiments be continued using the Kodiak radar. Specific experiments to determine the time required for irregularity generation and the heater power required should be carried out.

#### **4.7 Acknowledgements of Technical Assistance**

The crew at the HAARP facility has contributed in a large way to this work. Specifically, Dr. Mike McCarrick and Helio Zui have operated the heater for all of the experiments.

#### **4.8 Scientists and engineers who contributed to the research reported in this section.**

Dr. Paul Rodriguez of the Naval Research Laboratory, and Dr. Jim Sheerin of the University of Eastern Michigan have been the principal investigators for many of the experiments.  
Dr. William A. Bristow.

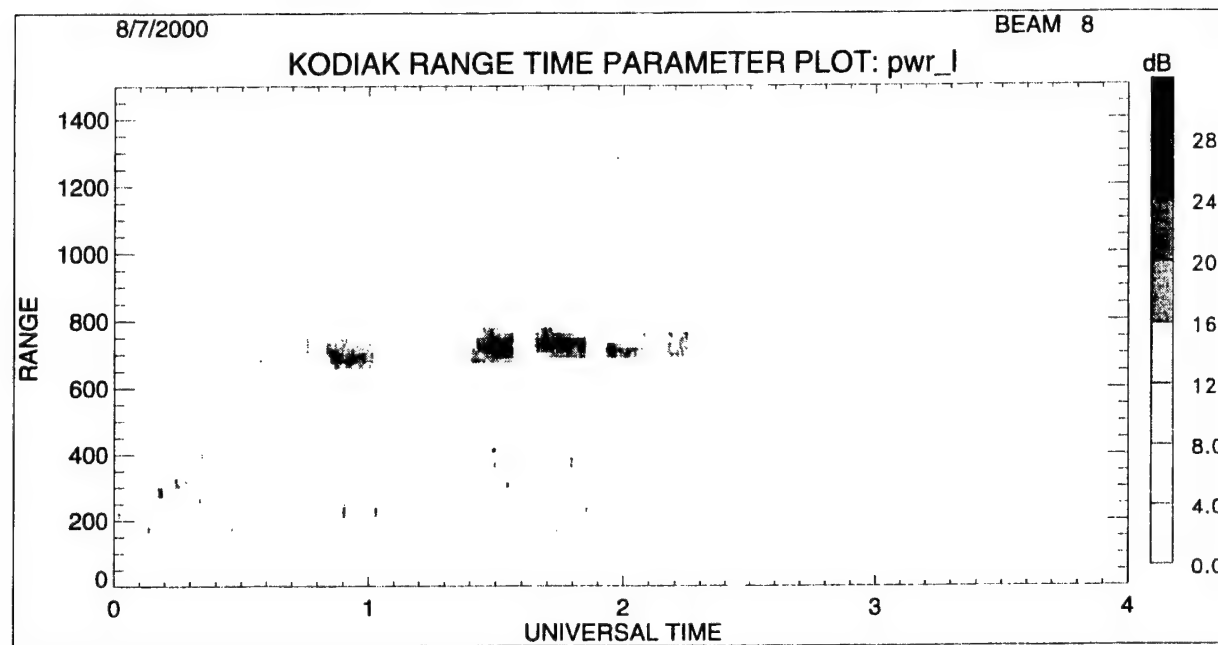


**Figure 16.** Power vs. range of radar scatter from August 7, 2000 between 0000 and 0400 UT.

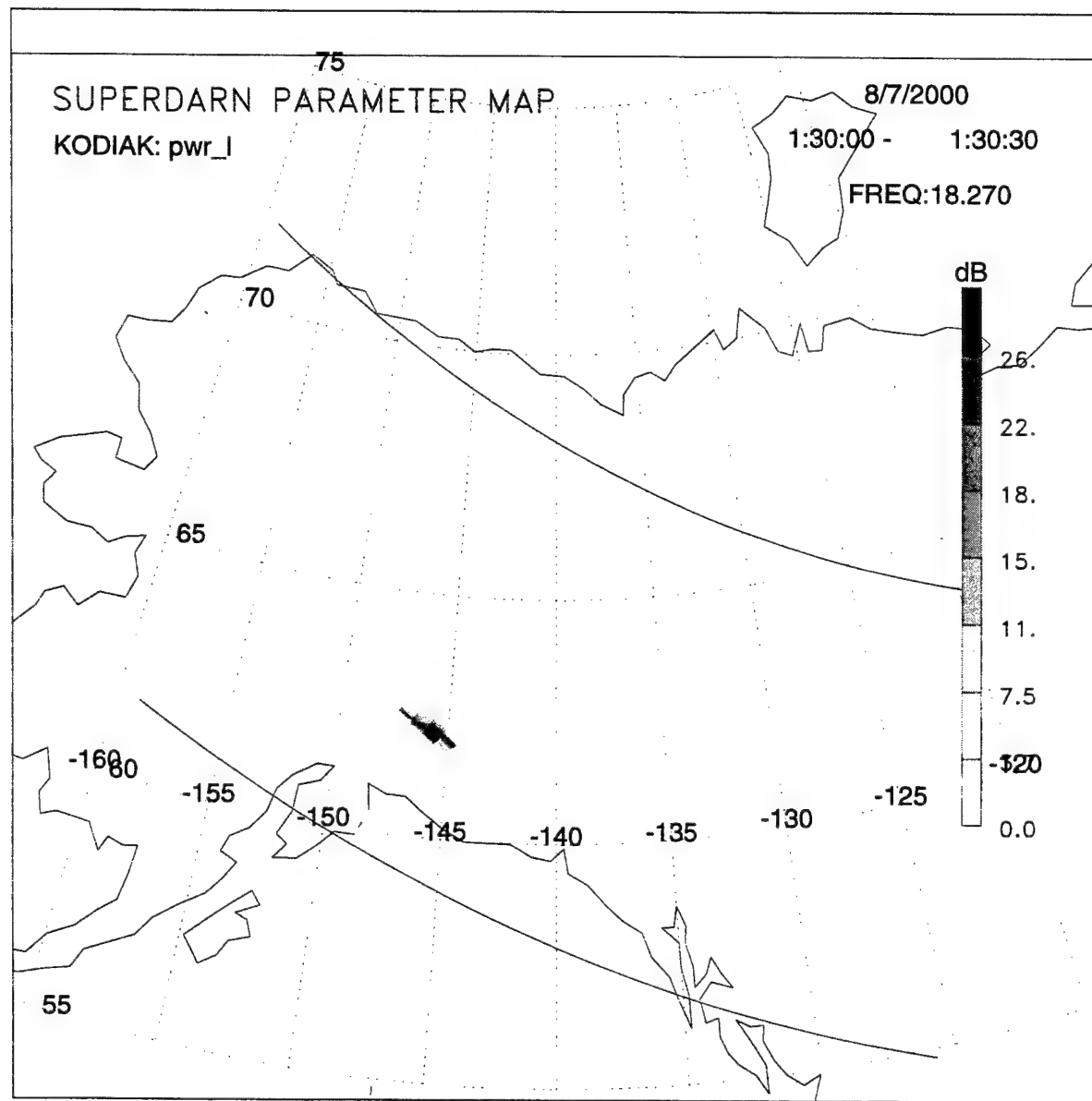


Figure 17. Geographic projection of scattered power at 0130 UT on August 7, 2000

## **5. Element 5: HAARP Science Outreach**

**Daniel J. Solie and John K. Petersen, Co-PIs**

### **5.1 Summary**

The HAARP Education Outreach program provides scientific education (about HAARP specifically and physical science in general) to members of the local Copper Valley community. This is done through direct involvement in local schools, public lectures and workshops, and intern and student research programs.

### **5.2 Introduction**

The chief objectives of the HAARP Science Outreach Program are to enhance science education opportunities in the Copper Valley, to educate local residents about the HAARP Research Program, and also to facilitate the direct involvement of students, teachers and the Copper Valley community in HAARP research campaigns and in the use of HAARP on-line data.

### **5.3 Methods, Assumptions and Procedures**

These objectives are accomplished through programs in the Copper Valley Schools and also in the local community. The school programs include: direct classroom involvement, workshops with K-12 teachers and encouraging high school appropriate research collaborations between HAARP researchers and interested students. The education programs for the larger community include physics demonstrations at the annual HAARP Open House, public lectures given by HAARP researchers and our participation in other community based science education programs.

### **5.4 Results and Discussion**

*The following is an abbreviated listing of the Education Outreach activity in the first 18 months:*

- Participation in annual HAARP Open House in Gakona, "Mr. Wizard" Science demonstrations (1999 & 2000)
- Sponsored HAARP Popular Lecture Series in cooperation with Prince William Sound Community College (Spring 2000, Fall 2000)
- Regular visits to give science presentations and involvement to public schools in the Copper Valley, including Chistochina School, Gakona School and Glennallen High School (Fall 1999 – Spring 2001)
- Presented a science workshop for public school teachers as part of a Copper Valley School District teacher training in-service (November 1999)
- Involvement in developing a Science Center in the Copper Valley (spring 2000 – present)
- Facilitation of Glennallen High School student/HAARP researcher research project (Fall 2000- present)

- Instigation of high school student summer intern program at HAARP (summer employment for a high school student in the Copper Valley at the HAARP site) (summer 1999 & summer 2000)
- Instigation of a HAARP university student intern program at UAF (summer 2000)

## **5.5 Conclusions**

All of the above activities require close cooperation with the Glennallen branch of the Prince William Sound Community College and the Copper Valley School District and also other members of the Glennallen community. In providing science outreach to outlying schools we are filling an important need in the rural schools. Judging from the feedback from local teachers, the children and parents we are accomplishing that goal. The public lectures, given by HAARP researchers, have two important functions: first they bring interesting science into the community, and second, they educate people on what kind of research is being done at HAARP. Attendance at the public lectures is growing. We plan to increase our outreach activity to more schools in the future as well as continue to provide workshops for teachers. The intern programs, especially the HAARP high school program, have been very successful. In the Copper Valley, our program is, to my knowledge, the only program specifically geared to the scientifically gifted student and thus serves an important role in educating scientists of the future.

## **5.6 Scientists and engineers who contributed to the research reported in this document.**

Dr. Daniel J. Solie and Dr. John K. Petersen

## REFERENCES

Fujita, S. (1987) Duct propagation of hydromagnetic waves based on the international reference ionosphere model, *Planet. Space Sci.*, **35**:91-103

Lanchester, B.S., Lummerzheim, D., Otto, A., Rees, M.H., Sedgemore-Schluthess, K.J.F., Zhu, H. and McCrea, I.W., (2001), Ohmic heating as evidence for strong field-aligned currents in filamentary aurora, *J. Geophys. Res.*, **106**:1785-179

von Stetten, David (1999) Propagation of Pc 1 pulsations in the ionospheric waveguide: A Review, Master's thesis, University of Alaska Fairbanks, Physics Dept.

Zhu, H., Otto, A., Lummerzheim, D., Rees, M.H. and Lanchester, B.S. (2001) Ionosphere-magnetosphere simulation of small-scale structure and dynamics, *J. Geophys. Res.*, **105**:1795-1806

## SYMBOLS, ABBREVIATIONS, ACRONYMS

AMT	Audio Magneto Telluric
CSAMT	Controlled Source Magneto Telluric
MHD	Magnetohydrodynamics
MSIS	Mass spectrometer incoherent scatter (model)
NCAR	National Center for Atmospheric Research
PEJ	Polar Electrojet
SEE	Stimulated electromagnetic emissions
SuperDARN	Super Dual Auroral Radar Network
TIME-GCM	Thermosphere ionosphere mesosphere electrodynamics general circulation model
UAF	University of Alaska Fairbanks
ULF	Ultra-low frequency